Hildebrand, C. E., Okinaka, R. T., & Heywood, P. (1975) *J. Cell Biol. 67*, 169a.
Hodge, L. D., Mancini, P., Davis, F. M., & Heywood, P. (1977) *J. Cell Biol. 72*, 194.
Kirby, K. S. (1968) *Methods Enzymol. 12B*, 87.
Kumar, A. (1970) *J. Cell Biol. 45*, 623.
Laemmli, U. K. (1970) *Nature (London) 227*, 680.
Leick, V., & Andersen, S. B. (1970) *Eur. J. Biochem. 14*, 460.
Liau, M. C., & Perry, R. P. (1969) *J. Cell Biol. 42*, 272.
Loening, U. E. (1969) *Biochem. J. 113*, 131.
Lowry, O. H., Rosebrough, W. H., Farr, N. L., & Randall, R. L. (1951) *J. Biol. Chem. 193*, 265.
Martin, T. E., & McCarthy, B. J. (1972) *Biochim. Biophys. Acta 277*, 354.
Miller, T. E., Huang, C. Y., & Pogo, A. O. (1978a) *J. Cell Biol. 76*, 675.
Miller, T. E., Huang, C. Y., & Pogo, A. O. (1978b) *J. Cell Biol. 76*, 692.
Monneron, A., & Bernhard, W. (1969) *J. Ultrastruct. Res. 27*, 266.
Narayan, K. S., Steele, W. J., & Busch, H. (1967) *Exp. Cell Res. 46*, 65.
Ogur, M., & Rosen, G. (1950) *Arch. Biochem. Biophys. 25*, 262.
Prescott, D. M., Bostock, C., Camow, E., & Lauth, M. (1971) *Exp. Cell Res. 67*, 124.
Prestayko, A. W., Tonato, M., & Busch, H. (1970) *J. Mol. Biol. 47*, 505.
Riley, D. E., & Keller, J. M. (1978) *J. Cell Sci. 29*, 129.
Riley, D. E., Keller, J. M., & Byers, B. (1975) *Biochemistry 14*, 3005.
Ro-Choi, T. S., & Busch, H. (1974) *Cell Nucl. 3*, 151–208.
Ro-Choi, T. S., Reddy, R., Henning, D., & Busch, H. (1971) *Biochem. Biophys. Res. Commun. 44*, 963.
Ronai, A., & Wunderlich, F. (1975) *J. Membr. Biol. 24*, 381.
Samarina, O. P., Lukanidin, E. M., Molnar, J., & Georgiev, G. P. (1968) *J. Mol. Biol. 33*, 251.
Shulman, R. W., Sripita, C. E., & Warner, J. R. (1977) *J. Biol. Chem. 252*, 1344.
Smetana, K., Steele, E. J., & Busch, H. (1963) *Exp. Cell Res. 31*, 198.
Wanka, F., Mullenders, L. H. F., Bekers, A. G. M., Pennings, L. J., Allen, J. M. A., & Eggensteyn, J. (1977) *Biochem. Biophys. Res. Commun. 74*, 739.
Warner, J. R. (1974) in *Ribosomes* (Nomura, M., Lengyel, P., & Tissières, A., Eds.) pp 461–488, Cold Spring Harbor Laboratories, Cold Spring Harbor, NY.
Weinberg, R. A., & Penman, S. (1969) *Biochim. Biophys. Acta 190*, 10.
Wunderlich, F. (1972) *J. Membr. Biol. 7*, 220.
Wunderlich, F. (1978) *Naturwiss. Rundsch. 31*, 282.
Wunderlich, F., & Herlan, G. (1977) *J. Cell Biol. 73*, 271.
Wunderlich, F., Berezney, R., & Kleinig, H. (1976) *Biol. Membr. 3*, 241–333.
Zieve, G., & Penman, S. (1976) *Cell 8*, 19.

Nitrogen-15 and Carbon-13 Dynamic Nuclear Magnetic Resonance Study of Chain Segmental Motion of the Peptidoglycan Pentaglycine Chain of ^{15}N-Gly- and $^{13}C_2$-Gly-Labeled *Staphylococcus aureus* Cells and Isolated Cell Walls†

Aviva Lapidot* and Charles S. Irving

ABSTRACT: The 9.12-MHz ^{15}N and 67.89-MHz ^{13}C NMR spectra were obtained for ^{15}N uniformly labeled *Staphylococcus aureus* and ^{15}N-Gly and $^{13}C_2$-Gly specifically labeled *S. aureus*. ^{15}N NMR measurements were made on normal intact cells, chloramphenicol-treated cells with thickened walls, partially autolyzed cells, and cell walls isolated from normal cells. ^{13}C NMR measurements were made on normal cells and cell walls and on partially autolyzed cell walls. The ^{15}N and ^{13}C intact-cell and cell wall spectra were dominated by resonances originating from N-terminal and nonterminal positions of the pentaglycine segment of the cell wall peptidoglycan. ^{13}C and ^{15}N NMR spectral parameters (T_1, line width, and NOE) could be accounted for by a log-χ^2 distribution of correlation times. The rapid, but highly correlated, chain motion of the pentaglycine bridge differed from that found in synthetic polymers and was characterized by shorter average correlation times and broader distributions of correlation times. The effect of temperature on the distribution of the correlation times was anomalous, with increasing temperature producing a wider distribution of correlation times. Chain motion of the pentaglycine bridge appeared to be dependent on the degree of packing of glycan strands rather than on noncovalent bonding interactions between adjacent peptide chains. Guanidine hydrochloride (6 M) had no effect on the spectral parameters of ^{15}N-Gly-labeled *S. aureus* cell walls. The anomalous temperature dependence of the distribution of correlation times could be accounted for by the transition from a flexible coil to a fully extended chain that accompanies the separation of the glycan strands and swelling of the cell wall. ^{15}N spectral parameters indicated that the degree of packing of the glycan strands is decreased by cell wall elongation and cell turgor.

The Gram-positive bacterial cell wall consists of an amphoteric polyelectrolyte gel of peptidoglycan and teichoic acid, whose main functions are to preserve the morphogenetically determined shape of the cell and to provide the fragile cytoplasmic membrane with the mechanical support needed to withstand the high osmotic pressures associated with hypotonic environmental conditions (Rogers, 1974; Shockman et al., 1974). The primary structures of peptidoglycan and teichoic

† From the Department of Isotope Research, Weizmann Institute of Science, Rehovot, Israel. *Received July 21, 1978; revised manuscript received November 19, 1978.* This work was presented in part at the 45th Annual Meeting of the Israel Chemical Society, Haifa, Israel, June 1978.

0006-2960/79/0418-1788$01.00/0

acids have been extensively studied (Ghuysen, 1968; Tipper, 1970; Coley et al., 1978). Due to the difficulties of making physical measurements on cell wall polymers under physiologically relevant conditions, many of the fundamental properties of the cell walls, such as the tertiary and quarternary structure of peptidoglycan, the degree of order in packing of cell wall polymers, and the nature of forces that help to maintain the morphogenetically determined arrangements of cell wall polymers, remain unknown (Rogers, 1974). A few attempts have been made to explain variations in the function and structural features of the cell wall in terms of the changes in the gel properties of the peptidoglycan–teichoic acid network (Marquis, 1968; Ou & Marquis, 1970, 1972). The absence of a comprehensive molecular model of the Gram-positive bacterial cell wall has made it difficult to define the molecular processes involved in cell wall elongation, changes in cell wall shape, and the action of antibiotics and autolysins on the cell wall.

Many of the spectroscopic techniques which have been used to characterize the conformations and dynamics of polypeptides and synthetic polymers are of little use in the study of complex biological systems, since they cannot distinguish between polymers in different cellular compartments. However, the recent observation (Lapidot & Irving, 1977b) of relatively intense ^{15}N nuclear magnetic resonance signals in cells and isolated cell walls originating from the pentaglycine bridge peptide of ^{15}N-Gly-labeled *Staphylococcus aureus* cell wall peptidoglycan has raised the possibility of using nuclear magnetic resonance measurements to probe the dynamic state of cell wall polymers.

We have prepared ^{15}N-labeled *S. aureus*, ^{15}N-Gly-labeled *S. aureus*, and $^{13}C_2$-Gly-labeled *S. aureus* and have measured the ^{15}N and ^{13}C T_1, T_2, and NOE values of the pentaglycine cross-bridge as a function of temperature, pH, guanidine hydrochloride, and autolysis.

The chain motions of the *S. aureus* peptidoglycan pentaglycine bridge were found to differ significantly from the motions of synthetic polymers. These qualitative features of the main chain motions of the cell wall polymers are interpreted in terms of flexible pentaglycine chains attached to immobile glycan strands, whose packing arrangements can vary as a function of temperature and growth conditions.

Materials and Methods

Labeled Reagent and Growth Medias. [^{15}N]Glycine was prepared (Schoenheimer & Ratner, 1938) from $H^{15}NO_3$ (95% ^{15}N) provided by the Isotope Separation Plant of the Weizmann Institute. [$^{13}C_2$]Glycine was obtained from Merck Sharp & Dohme Isotopes, Canada. The [^{15}N]amino acid mixture was obtained from the protein hydrolysate of Baker's yeast grown at 37 °C with aeration on glucose (6 g/L), Difco carbon base (10 g/L), and Spizizen minimal salts media (Spizizen, 1958), in which $(NH_4)_2SO_4$ (2 g/L) was replaced by $^{15}NH_4Cl$ (1 g/L). ^{15}N-Gly-labeled *S. aureus* and $^{13}C_2$-Gly-labeled *S. aureus* were grown on McVeigh–Hobdy media (McVeigh & Hobdy, 1952) in which glycine in the synthetic amino acid mixture was replaced by [$^{13}C_2$]glycine (150 mg/L) and [$^{13}C_2$]glycine (150 mg/L), respectively. ^{15}N-Labeled *S. aureus* was grown on McVeigh–Hobdy media (McVeigh & Hobdy, 1950) in which the synthetic amino acid mixture was replaced by the [^{15}N]amino acid mixture (1 g/L).

Preparation of Cell and Cell Wall Samples. S. aureus was grown at 37 °C with gyrorotatory shaking and aeration in 5-L conical flasks containing 1 L of growth media. Cell growth was followed by measurement of extinction at 675 nm by means of a side arm fixed to the growth flask and continued into the mid-log growth phase (OD_{675} 0.1–0.15). Upon completion of growth, 4% $NaDodSO_4$[1] was added to the growth media to inactivate autolysins (Rogers & Forsberg, 1971), and shaking was continued for 10 min at 37 °C, after which time the bacterial cells were rapidly harvested by centrifugation (Sorval RC2-B rotor; 10000*g*; 10 min) at 37 °C. The cell pellet was washed three times with distilled water at 37 °C to remove traces of $NaDodSO_4$. Cell walls were prepared by mechanical disruption of cells in a Braun tissue homogenizer by shaking at maximum speed with 0.1–0.11-nm diameter ballatoni glass beads (B. Braun Melsungen, West Germany; No. 541540) for 3 min at 4 °C. The supernatant was decanted from the glass beads and centrifuged (1000*g*; 10 min) to remove unbroken cells. Cell walls were obtained from the resulting supernatant by centrifugation (15000*g*; 10 min), and the pH was adjusted to pH 7 by addition of concentrated HCl when needed.

Partially autolyzed cells were obtained by harvesting *S. aureus* in mid-log growth phase without prior inactivation of cell wall autolysins by $NaDodSO_4$ treatment. To obtain partially autolyzed cell walls, the cell walls of cells that were harvested without $NaDodSO_4$ inactivation of autolysins were incubated at pH 9.0, 37 °C, for 5–10 h and then were washed three times with distilled water, and the pH was adjusted by addition of concentrated HCl. Thick-wall *S. aureus* cells were prepared by blocking protein synthesis by addition of chloramphenicol (50 μg/mL) to cells in the early log growth phase (OD_{675} 0.05–0.1); shaking with aeration was continued at 37 °C for 2 h, and cells were treated with $NaDodSO_4$ and harvested in the usual manner.

Intact cells and isolated cell walls were packed into 10-mm NMR tubes (Wilmad; No. 513-7pp) to heights of 2 to 2.5 cm by centrifugation at 3000 rpm (IEC HN-S centrifuge) for 0.5 and 2 h, respectively. The dry weights of the intact cell and cell wall samples were ~300 and ~100 mg, respectively.

NMR Measurements. ^{15}N NMR experiments were performed on a Brucker WH-90 pulse Fourier transform spectrometer operating at 9.12 MHz. Fourier transformed proton broad-band noise-decoupled spectra consisting of 2K data points were obtained with the following spectrometer conditions: 90° pulse angle of 28-μs duration, 2-kHz spectral width, 10000 accumulations, 2-Hz exponential filter, and 0.976-Hz digital resolution.

Field stabilization was accomplished by locking on the deuterium resonance of D_2O in a 5-mm concentric tube inserted into the 10-mm sample tube. A sample of 4 M $^{15}NH_4Cl$ in 2 M HCl in a 2-mm concentric tube inserted into the 5-mm tube of D_2O provided an external reference signal at 350.89 ppm upfield from $H^{15}NO_3$. Chemical shifts are estimated to be accurate to ±0.05 ppm.

^{13}C NMR experiments were performed on a Brucker WH-270 pulse Fourier transform spectrometer operating at 67.899 MHz. Fourier transformed proton broad-band noise-decoupled spectra consisting of 8K data points were obtained with the following spectrometer conditions: 90° pulse angle of 18-μs duration, 15-kHz spectral width, 2000 accumulations, 1-Hz exponential filter, and 1.849-Hz digital resolution. Field stabilization was provided by a 5-mm concentric tube containing D_2O, while a 2-mm concentric tube containing dioxane provided an external reference at 66.7 ppm downfield from Me_4Si.

[1] Abbreviations used: GlcNAc, *N*-acetylglucosamine; Gdn·HCl, guanidine hydrochloride; *meso*-DAP, *meso*-diaminopimelic acid; MurNAc, *N*-acetylmuramic acid; NMR, nuclear magnetic resonance; $NaDodSO_4$, sodium dodecyl sulfate.

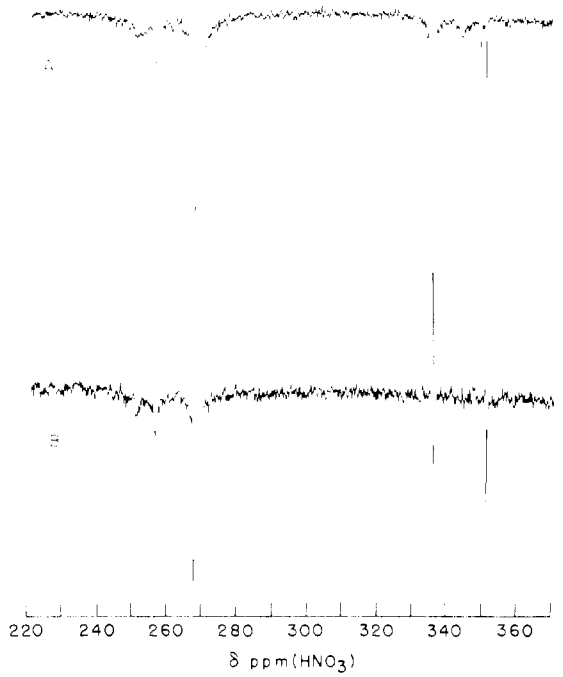

FIGURE 1: Proton-decoupled 9.12-MHz ^{15}N NMR spectra at 27 °C of ^{15}N-labeled *S. aureus* whole cells (A) and isolated cell walls (B).

Sample temperatures were maintained by a Brucker temperature-control unit and measured directly by immersion of the thermocouple into the 5-mm concentric tube containing D_2O.

To obtain the chemical shifts, half-height line widths, and relative intensities of overlapping ^{15}N or ^{13}C glycyl resonances, the resonance band shapes were simulated by the superposition of Lorentzian-shaped lines with variable heights, half-height line widths, and chemical shifts, by using interactive graphics computer programs written in SPEAKEZ. Best fits were judged by visual comparison of experimental and simulated band shapes on an Tektronic 4014 visual display unit. Chemical shifts, line widths, and relative intensitives are accurate to ±0.05 ppm, 20%, and 5%, respectively.

Determination of Spectral Parameters. T_1 values were determined from inversion-recovery relaxation experiments with a standard $D - 180° - \tau - 90°$ pulse sequence where the delay, D, was 3 s for normal cells and cell walls and 10 s for autolyzed cell walls. Partially relaxed ^{15}N and ^{13}C spectra consisted of 1000 and 300 free induction decays, respectively. Five to ten values of τ were used in each T_1 determination. T_1^{-1} values were obtained from the slopes of ln $[(A_\infty - A_\tau)/A_\infty]$ vs. τ least-squares lines, where A is the area of the computer-simulated Lorentzian-shaped resonance. Errors in the slope, evaluated at the 95% confidence level, were carried over into the determination of T_1 values. T_2 values were calculated from half-height line widths [lw = $1/(\pi T_2)$] of computer-simulated resonances that were corrected for instrumental and digital broadening (0.5–2 Hz). NOE values were determined from the ratio of the areas of computer-simulated resonances of proton broad-band noise-decoupled and gated-decoupled spectra obtained from 10000 ^{15}N and 2000 ^{13}C free induction decays. In gated-decoupled measurements, delays of at least $10T_1$ were used and broad-band proton decoupling was on only during the aquisition of the free induction decays. The use of shorter delays ($<10T_1$) in ^{15}N gated-decoupled measurements resulted in significantly attenuated resonances.

Results

^{15}N-Labeled S. aureus. The proton-decoupled, 9.12-MHz ^{15}N NMR spectra of ^{15}N uniformly labeled *S. aureus* intact cells and isolated cell walls (Figure 1) display relatively narrow (~5–30 Hz), inverted ^{15}N resonances at 250.2–251.7 (alanine), 255.7 (Lys-N_ω), and 267.3 ppm (glycine) in the amide region and resonances at 336.6 (teichoic acid and D-Ala), 343.9 (Lys-N_ω), and 349.2 ppm (glycine) in the amino region, in addition to the $^{15}NH_4Cl$ external reference signal at 350.89 ppm. The qualitative similarity of intact cell and isolated cell wall spectra indicates that the ^{15}N resonances originating from cell wall components dominate the intact-cell spectra. Assignments to particular types of amino acid groups are based on previously reported specific isotope labeling experiments (Lapidot & Irving, 1978, 1979).

The 267.3- and 349.2-ppm resonances are assigned to nonterminal and N-terminal glycyl residues, respectively. The assignments of glycyl resonances to various types of monomeric, cross-linked, and autolyzed peptidoglycan peptide chains (Figure 2) (Ghuysen, 1968) are less straightforward. The absence of a C-terminal glycyl peptide resonance at 260.3 ppm indicates that the nonterminal glycyl resonance at 267.3 ppm does not originate from peptide chains with cleaved Gly–Gly or Gly–Ala peptide bonds. The absence of γ-D-Glu (253.4–254.2 ppm) and L-Lys-Nω (256.5 ppm) resonances indicates that cross-linked peptide chains with one autolyzed MurNAc–L-Ala bond do not contribute to the nonterminal glycyl peptide resonance (Irving & Lapidot, 1978a,b). The

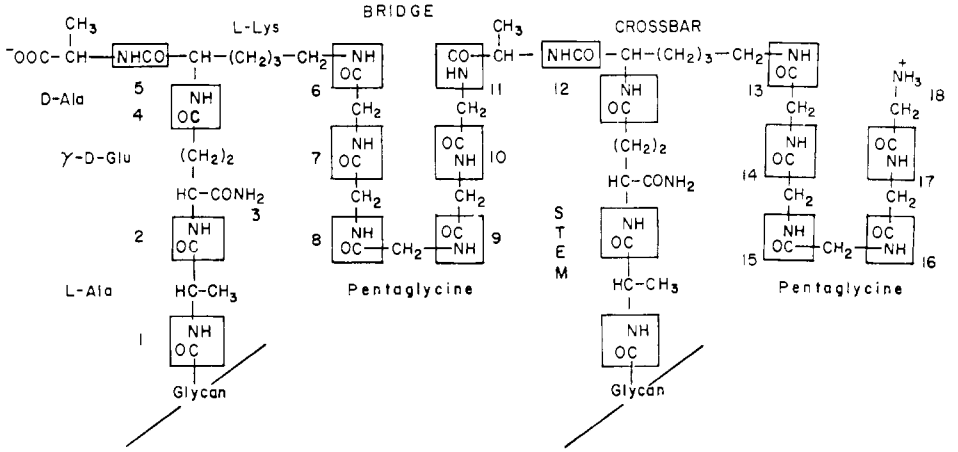

FIGURE 2: Primary structure of the peptide chains of *S. aureus* cell wall peptidoglycan according to Ghuysen (1968). The different types of peptide nitrogens are marked and numbered for reference. Cleavage of the Gly–Ala bond at position 11 yields the C-terminal Ala residue at position 5 and the non-cross-linked pentaglycine chain at positions 14–18. The peptide chain is divided into stem, crossbar, and bridge regions according to Oldmixon et al. (1974).

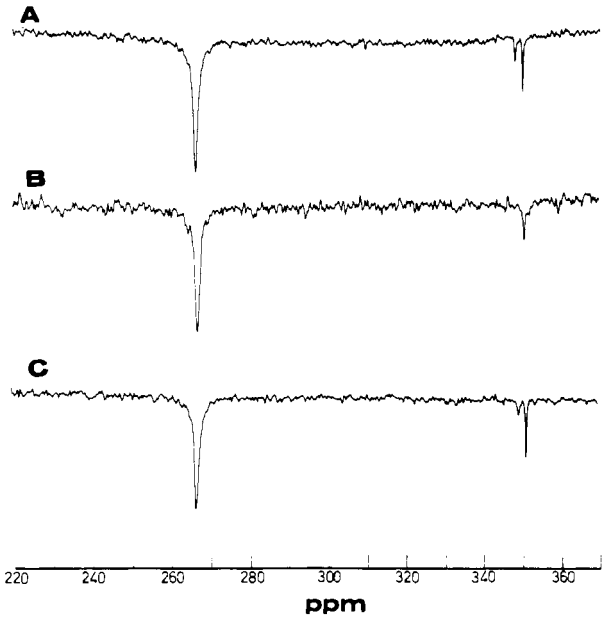

FIGURE 3: Proton-decoupled 9.12-MHz ^{15}N spectra of ^{15}N-Gly-labeled *S. aureus* cells. (A) Normal cells at 28 °C; (B) normal cells at 7 °C which may have been partially autolyzed due to the omission of $NaDodSO_4$ inactivation of autolysins before harvesting; (C) cells at 28 °C with thickened cell walls resulting from chloramphenicol inhibition of cell elongation and protein synthesis.

relatively small integrated area of the N-terminal glycyl free amino resonance (349.3 ppm) compared to the nonterminal peptide resonance (267.3 ppm) indicates that monomeric peptide chains (regions 14–18 of Figure 2) by themselves cannot account for the intensity of the nonterminal glycyl resonance. We conclude that the nonterminal glycyl peptide resonance originates largely from cross-linked peptide chains (regions 7–11 of Figure 2). In order to avoid the possible overlap of the 266.8-ppm amide NH_2 resonance of amidated γ-D-Glu residues (3 in Figure 2) with nonterminal glycyl peptide resonance, all subsequent ^{15}N NMR measurements were made on *S. aureus* specifically labeled in the glycyl residues.

^{15}N-Gly-Labeled S. aureus. The high absolute intensity of the nonterminal glycyl peptide ^{15}N resonance, that results from the large mass of the cell wall (20% dry weight of the cell) and the high percentage of glycyl groups in the cell wall (Salton, 1964), allows (Lapidot & Irving, 1977b) gated-decoupled and inversion-recovery ^{15}N NMR experiments to be made on the nonterminal glycyl resonance. The proton-decoupled ^{15}N NMR spectra of ^{15}N-Gly-labeled *S. aureus* cells and cell walls (Figure 3) display, in addition to the free amino glycyl resonance (349.3 ppm), an intense band at 267.3 ppm, which consists of a Lorentzian-shaped line with a half-height line width of ~11 Hz superimposed on a broader degenerate resonance, whose signal amplitude was about 5% of the major resonance (Figure 4). Due to noise levels at the base of the resonance, it was not possible to decide whether the low-intensity resonance, whose line width was about 50 Hz, is a single Lorentzian-shaped line or an envelope of resonances. All subsequent measurements were restricted to the major resonance. A typical ^{15}N gated-decoupled spectrum is shown in Figure 4.

Comparison of the proton-decoupled ^{15}N NMR spectra of normal, chloramphenicol-treated, and $NaDodSO_4$-nontreated ^{15}N-Gly-labeled *S. aureus* intact cells (Figure 3) did not reveal any changes in the band shape or chemical shift of the pentaglycine bridge resonance. However, the T_1, T_2, and NOE

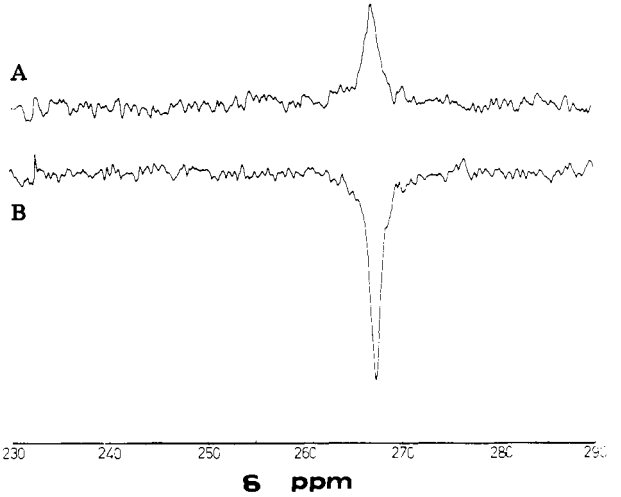

FIGURE 4: Proton gated-decoupled (A) and broad-band noise-decoupled (B) 9.12-MHz ^{15}N NMR spectra of ^{15}N-Gly-labeled *S. aureus* cells.

Table I: Observed Relaxation Parameters of Pentaglycine Cross-Bridge ^{15}N Resonance in ^{15}N-Gly-Labeled *S. aureus* Cells and Cell Walls

system	T (K)	T_1 (ms)	T_2 (ms)	NOE
normal cells	301	426 ± 29	30	−2.05
thick-wall cells (chloramphenicol)	301	310 ± 52	27	−1.63
autolyzed cells	280	301 ± 68	23	
normal cell walls	278	260 ± 11	29	
	303	380 ± 38	29	−2.67
	323	654 ± 98	33	
normal cell walls in 6 M Gdn·HCl	277	238 ± 25	28	
	301	364 ± 54	28	−2.76
	323	770 ± 30	30	

values of the three types of cell samples (Table I) did show significant differences. Inhibition of protein synthesis by chloramphenicol, which blocks cell wall elongation and leads to thickening of the cell wall and inhibition of cell wall autolysis (Roger & Forsberg, 1971), resulted in shorter T_1 relaxation times and smaller NOE values compared to those of normal cells. ^{15}N-Gly-labeled *S. aureus* cells, which had not been treated with $NaDodSO_4$ prior to harvesting to inactivate autolysins, had shorter T_1 and T_2 relaxation times, compared to normal cells, when values measured at 280 K are extrapolated to 301 K (see below). The T_1, T_2, and NOE values of major pentaglycine bridge resonance of isolated cell walls obtained from normal ^{15}N-Gly-labeled *S. aureus* were slightly smaller than the values of the normal intact cells (Table I).

Transfer of normal cell walls from an aqueous environment to 6 M guanidine hydrochloride had practically no effect on the T_1, T_2, and NOE values and their temperature dependencies when compared to normal cell walls in an aqueous suspension (Table I).

The T_1, T_2, and NOE values of the glycyl free amino resonance were not studied due to the low signal amplitude and the long T_1 relaxation times of the free amino glycine resonance and the remarkable sensitivity of the T_1 and NOE values to trace amounts of paramagnetic impurities (Irving & Lapidot, 1975). However, the spectral parameters of N-terminal and nonterminal glycyl residues could be compared by using the ^{13}C NMR resonance of *S. aureus* specifically labeled with glycine enriched at the C_2 position.

$^{13}C_2$-Gly-Labeled S. aureus. The proton-decoupled 67.89-MHz ^{13}C NMR spectrum of $^{13}C_2$-Gly-labeled *S. aureus*

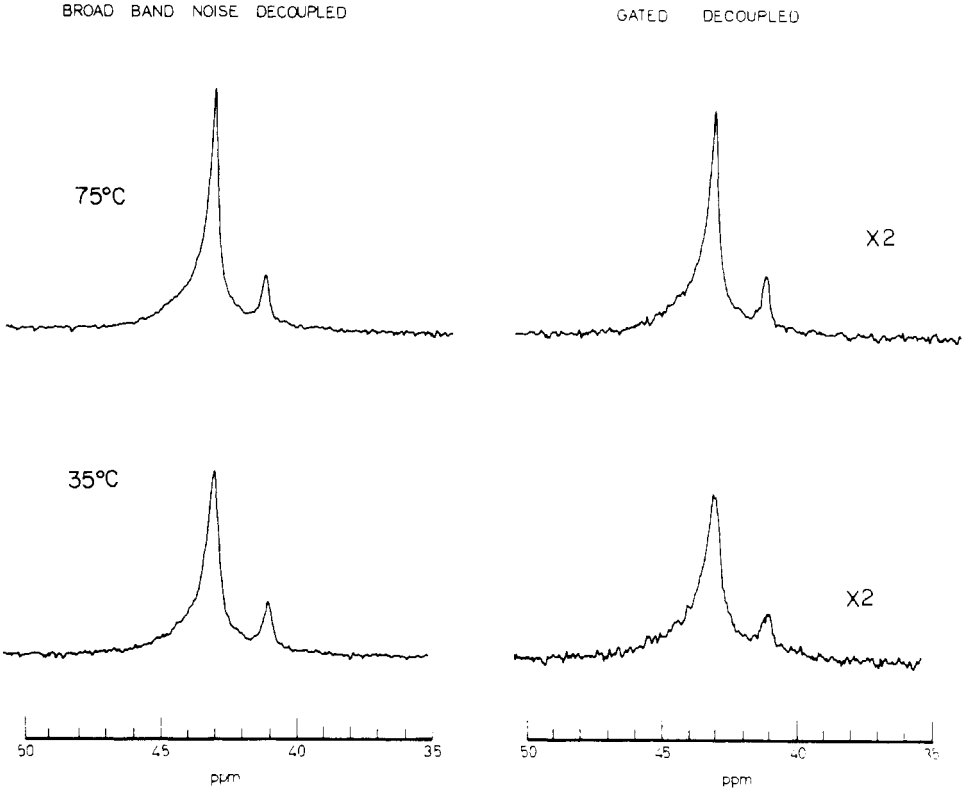

FIGURE 5: Observed proton broad-band noise-decoupled (left) and gated-decoupled (right) 67.889-MHz ^{13}C NMR spectra of $^{13}C_2$-Gly-labeled *S. aureus* cell walls at 75 °C (upper) and at 35 °C (lower).

FIGURE 6: Inversion-recovery measurement using a $D - 180° - \tau - 90°$ pulse sequence of the T_1 values of the three cell wall ^{13}C resonances of $^{13}C_2$-Gly-labeled *S. aureus* cell walls at 35, 55, and 75 °C. Signal amplitudes were obtained from computer-simulated band shapes (not shown). A delay, D, of 4 s ($>5T_1$) was used in each measurement.

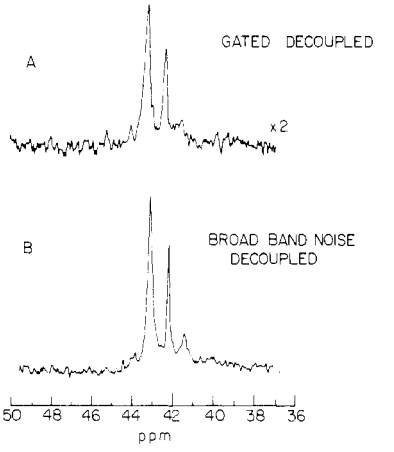

FIGURE 7: Proton gated-decoupled (A) and broad-band noise-decoupled (B) 67.889-MHz ^{13}C NMR spectra of partially autolyzed $^{13}C_2$-Gly-labeled *S. aureus* cell walls at 29 °C, pH 7.0. Partially autolyzed cell walls were prepared by incubating at pH 9.0 and 37 °C for 5 h. *S. aureus* cell walls were obtained from cells which had not been treated with $NaDodSO_4$.

cells (Figure 5) displays an intense, asymmetric resonance centered at 43 ppm, which consists of four Lorentzian lines, at 40.0, 41.4, 43.0, and 43.7 ppm, whose relative intensities and T_2 values are given in Table II, along with the T_1 values of the major resonance at 43.0 ppm. The ^{13}C NMR spectrum of isolated cell walls of $^{13}C_2$-Gly-labeled *S. aureus* also displayed an intense asymmetric resonance centered at 43 ppm which consisted of three Lorentzian-shaped lines at 41.1, 43.0, and 43.7 ppm (Figure 6). The absence of the 40.0-ppm resonance in the cell wall spectrum suggested that this resonance originated from a cytoplasmic component. All subsequent ^{13}C NMR measurements were restricted to the isolated cell walls. The T_1, T_2, and NOE values and gated-decoupled relative intensities of the three glycyl ^{13}C resonances of the cell wall, measured at three temperatures, are given in Table II. The partially relaxed spectra of the $^{13}C_2$-Gly-labeled *S. aureus* cell walls at three temperatures are shown in Figure 6. Partial autolysis of $^{13}C_2$-Gly-labeled *S. aureus* cell walls leads to a 0.3-ppm downfield shift of the 41.1-ppm resonance, an increase in the T_1, T_2, and NOE values, a change in relative intensities of the three cell wall resonances, and the appearance of a new resonance at 42.0 ppm, with a long T_1 relaxation time of 2.4 s (Figure 7 and Table II).

Cell wall resonances can be assigned to terminal and nonterminal glycyl groups on the basis of their pH titration shifts (Christl & Roberts, 1972; Keim et al., 1972, 1974). Chemical shifts of the 43.0-and 43.7-ppm resonances are insensitive to pH, while the 41.4-ppm resonance shifts 3.4 ppm downfield at pH 11.0 (Figure 8). Both the chemical shift and the pH titration shifts of the 41.4-ppm resonance are char-

Table II: Observed Relaxation Parameters of Pentaglycine Cross-Bridge ^{13}C Resonances in $^{13}C_2$-Gly-Labeled *S. aureus* Cells and Cell Walls

system	resonance	T (K)	rel area	T_1 (ms)	T_2 (ms)	NOE
normal intact cells	40.0	303	1.0		2.1	
	41.2	303	1.0		10.6	
	43.0	303	4.50		7.1	
	43.5	303	8.00		1.6	
normal cell walls	41.1	308	1.0	203 ± 21	10.6	2.05
		328	1.0	446 ± 20	15.9	2.0
		348	1.0	(870)	14.5	1.6
	43.0	308	4.5	142 ± 5	7.9	2.2
		328	4.8	202 ± 4	12.7	2.12
		348	4.4	360 ± 10	11.8	2.1
	43.7	308	6.1	96 ± 2	2.1	1.25
		328	6.2	101 ± 8	2.1	1.79
		348	7.2	125 ± 6	2.1	1.80
partially autolyzed cell walls	41.4	308	1.0	444 ± 43	32	2.4
	42.0	308	5.1	2405 ± 196	42	2.5
	43.0	308	8.1	174 ± 7	23	2.3
	43.7	308	1.0		22	3.0

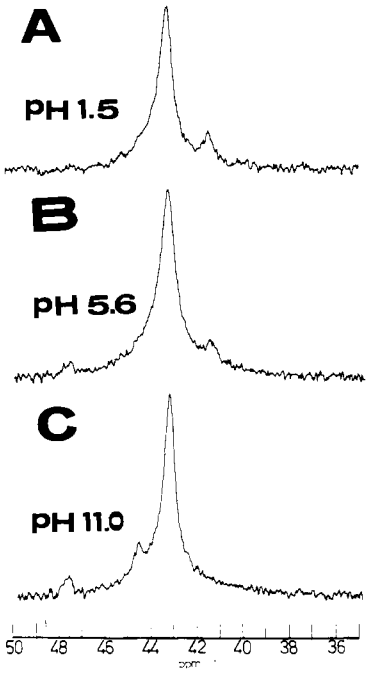

FIGURE 8: Proton-decoupled 67.889-MHz ^{13}C NMR spectra at 29 °C of normal $^{13}C_2$-Gly-labeled *S. aureus* cell walls at pH 1.5 (A), 5.6 (B), and 11.0 (C).

acteristic of an N-terminal glycyl residue. The absence of a C-terminal glycyl ^{13}C resonance is consistent with the ^{15}N NMR results. The 43.0- and 43.7-ppm resonances can be assigned to two types of nonterminal glycyl residues. Nearest-neighbor effects (Christl & Roberts, 1972) are too small to account for the 0.7-ppm difference in chemical shifts of the C_2 glycyl carbons. The ^{13}C chemical shifts of glycyl residues with hindered internal rotations (43.4–43.6 ppm) (Tancrede et al., 1978) occur downfield from glycyl residues in random coils (42.0–42.8 ppm) (Chien & Wise, 1973; Glusko et al., 1972). It is reasonable that two nonterminal glycyl resonances originate from peptide chains with hindered motion and that the 43.7-ppm resonance corresponds to a glycyl group whose internal rotations are more hindered than those of the 43.0-ppm group. This is consistent with the decrease in the relative intensity of the 43.7-ppm resonance and the increase in the relative intensity resonance of the 43.0-ppm resonance following autolysis of the cell wall. However, it is not possible at present to distinguish between two types of resonances corresponding to different sites in the same type of peptide chain from glycyl residues in two types of different peptide chains, such as monomeric and cross-linked pentaglycine bridges. The 4.5:1.0 ratio of nonterminal 43.0-ppm resonance to the C-terminal glycyl resonance found in the normal cell wall would be consistent with the assignment of the 43.0-ppm resonance to the four nonterminal glycyl residues in the non-cross-linked pentaglycine bridge (regions 13–17 in Figure 2); however, the ratio does not remain constant in the autolyzed cell walls, where it increases to 8:1.

Discussion

Chain Motions. As a result of the attachment of peptidoglycan peptide chains to relatively immobile glycan strands, the molecular motion of the peptidoglycan pentaglycine bridge results entirely from local segmental motions, in contrast to the situation in peptides and proteins where both overall isotropic reorientations and internal rotations contribute to molecular motion of peptide groups. The observation of relatively intense glycyl ^{15}N and ^{13}C NMR resonances in the *S. aureus* cell wall indicates that a sizable fraction of peptidoglycan pentaglycine bridges undergoes rapid segmental motions. ^{15}N chemical shifts of peptide nitrogens are remarkably sensitive to conformational and solvation effects (Llinas & Wüthrich, 1978; Markowski et al., 1977; Hawkes et al., 1976), and in native hemoglobin, glycyl ^{15}N resonances are spread over a 20-ppm range (Lapidot & Irving, 1977a). The observation of a single, major, Lorentzian-shaped resonance in *S. aureus* cell wall indicates that internal segmental motions have averaged out differences in solvation and conformation along the pentaglycine chain. In order to better characterize the nature of the local segmental motions, we have examined the T_1, T_2, and NOE values of the cell wall ^{15}N and ^{13}C NMR resonances in terms of the models of chain segmental motions which have recently been applied to ^{13}C relaxation data of polypeptides, polysaccharides, and synthetic polymers (Lyerla & Torchia, 1975; Torchia & Vander Hart, 1976; Torchia et al., 1977; Schaefer, 1973; Heatley & Begum, 1976; Lyerla et al., 1977; Levy et al., 1978).

The T_1, T_2, and NOE values of ^{15}N and ^{13}C groups that relax via dipolar interactions with directly attached protons are given by (Abragam, 1961; Lyerla & Levy, 1974)

$$\frac{1}{T_1} = \frac{1}{10}N\frac{\gamma_I^2\gamma_H^2}{r^6}[J(\omega_I - \omega_H) + 3J(\omega_I + \omega_H)] \quad (1)$$

$$\frac{1}{T_2} = \frac{1}{20}N\frac{\gamma_I^2\gamma_H^2}{r^6}[J(\omega_I - \omega_H) + 3J(\omega_I) + 6J(\omega_I + \omega_H) + 4J(0) + 6J(\omega_H)] \quad (2)$$

$$\text{NOEF} = \text{NOE} + 1 = \frac{\gamma_H}{\gamma_I}\left[\frac{-J(\omega_I - \omega_H) + 6J(\omega_I + \omega_H)}{J(\omega_I - \omega_H) + 3J(\omega_I) + 6J(\omega_I + \omega_H)}\right] \quad (3)$$

where γ is the gyromagnetic moment, ω is the Lanmor frequency, I refers to either ^{13}C or ^{15}N, r is the NH (0.9 Å) or CH_2 (1.09 Å) bond length, N is the number of directly attached protons, and $J(\omega)$ is the spectral density function.

The extent to which the pentaglycine chain motions can be described by a single, isotropic reorientation correlation time, τ_r, has been determined by calculating the τ_r values which yield the observed T_1, T_2, and NOE values of cell wall ^{13}C and ^{15}N resonances, by using the isotropic reorientation correlation function $J(\omega) = \tau_r/(1 + \tau_r^2\omega^2)$ (Lyerla & Levy, 1974; Abragam, 1961). Very different τ_r values are obtained from T_1, T_2, or NOE values of a single resonance at a single temperature. Thus isotropic overall reorientation is not a useful or meaningful model for this system. This is not the case for native globular proteins and unfolded random-coil proteins and oligopeptides, whose spectral parameters can be accounted for by a single isotropic rotational correlation (Egan et al., 1977). However, this situation has been noted in ^{13}C NMR studies for isotactic polystyrene, *cis*-polyisoprene, and *cis*-polybutadiene (Schaefer, 1973, 1974), for poly(propylene oxide), polystyrene, and atactic poly(methyl methacrylate) (Heatley & Begum, 1976), for isotactic and syndiatactic poly(methyl methacrylate) (Lyerla et al., 1977), for elastin (Lyerla & Torchia, 1975), and for proteoglycan (Torchia et al., 1977).

The log–χ^2 distribution introduced by Schaefer (1973) has proved useful in describing the distribution of correlation times in the backbone motions of polymer chains and in accounting for the effects of temperature, tacticity, and chain entanglements on the degrees of freedom of the chain motion. In the log–χ^2 distribution, a logarithmic time scale in defined by

$$S = \log_b [1 + (b - 1)\tau/\bar{\tau}] \quad (4)$$

where b is an adjustable parameter, usually taken to be 1000. The distribution function is given by

$$H(s) = \frac{1}{\Gamma(p)}(ps)^{p-1}e^{-ps}p \quad (5)$$

where p is the width parameter and $\Gamma(p)$ is a normalization factor and is equal to the Γ function of p. The width parameter, p, is a measure of the degrees of motional freedom, and at $p > 100$ the function is equivalent to a single correlation time equal to τ. The spectral density function for the log–χ^2 distribution is given by

$$J(\omega) = \int_0^\infty \frac{\bar{\tau}H(s)(\exp_b s - 1)}{(b - 1)\{1 + \omega^2\bar{\tau}^2[(\exp_b s - 1)/(b - 1)]^2\}}ds \quad (6)$$

which can be evaluated numerically. If the model applies, three independent values of T_1, T_2, and NOE can be accounted for by the two adjustable parameters p and $\bar{\tau}$.

Both the qualitative and quantitative features of the T_1, T_2, and NOE cell wall ^{13}C data can be fitted at all temperatures by a log–χ^2 distribution model, as seen in Table III. The $\bar{\tau}$ values obtained for the 41.1- and 43.0-ppm resonances fall in the range of τ_{int} values reported for the Gly-2 residue of enkephalin (Tancrede et al., 1978). Arrhenius plots for $\bar{\tau}$ or $1/T_1$ are nonlinear and had activation energies between 12 and 60 kJ/mol.

However, "simple" activation energies may have little physical significance, since the width of the distribution varies with temperature (Levy et al., 1978).

Table III: Correlation Times, Distribution Width Parameters, and Predicted Relaxation Parameters for the $^{13}C_2$-Gly-Labeled *S. aureus* Cell Wall[a]

resonance	T (K)	distribution width p	correlation time, τ (ns)	predicted ^{13}C parameters T_1 (ms)	T_2 (ms)	NOE
41.1	308	7	0.07	203	10.6	2.05
	328	3	0.01	388	16.4	1.93
43.0	308	8	0.20	145	6.7	1.93
	328	7	0.070	203	12.5	2.01
	348	3	0.015	351	11.9	1.92
43.7	308	10	1.4	95	2.1	1.68
	328	9	1.0	102	2.0	1.74
	348	8	0.4	123	3.4	1.85

[a] Calculated by use of the log–χ^2 distribution with $b = 1000$.

The p and $\bar{\tau}$ values (Table III) obtained for ^{13}C spectral parameters of the pentaglycine bridge differ significantly from those reported for synthetic polymers. The $\bar{\tau}$ values of the pentaglycine bridge are considerably smaller than those of the backbone carbons of synthetic polymers. The $\bar{\tau}$ values of pentaglycine fall on the high-frequency side of the T_1 minimum, whereas the $\bar{\tau}$ values of synthetic polymers occur on the low-frequency side. The segmental motions are more correlated than those found in synthetic polymers and are described by smaller p values. The most pronounced difference is the increase in the width of the distribution and degree of correlation of pentaglycine chain motions with increasing temperature. In synthetic polymers, the distributions are narrower at elevated temperatures as the freedom of motion increases.

Comparison of the τ and p values of the three cell wall glycyl ^{13}C resonances shows that the 43.0-ppm nonterminal glycyl resonance and the 41.1-ppm N-terminal glycyl resonance have similar $\bar{\tau}$ values, activation energies, width parameters, and variations of width parameters with temperature. The similarity of the ^{13}C spectral parameters of the two resonances suggests that they may originate from similar types or regions of pentaglycine chains. The 43.7-ppm nonterminal glycyl resonance originates from a chain segment, whose segmental motions are slower (as indicated by $\bar{\tau}$ values) and less correlated and have lower energies of activation.

Other models for chain segmental motions were also investigated. The qualitative features of the ^{13}C data could also be accounted for by Cole–Cole distributions (Heatley & Begum, 1976). It should be noted that good fits of the cell wall ^{13}C data could *not* be obtained when the conformational jump spectral density functions given by Heatley & Begum (1976) were used.

The ^{15}N cell wall data of the major nonterminal glycyl resonance resemble the ^{13}C data in several respects. The ^{15}N T_1 values increase with temperature (Table I) and correspond to relatively short average correlation times. The peculiar set of ^{15}N T_1, T_2, and NOE values could not be accounted for by either Cole–Cole, conformation jump, or ellipsoidal rotation spectral density functions (Heatley & Begum, 1976). The τ_r values obtained from ^{15}N data when the single rotational correlation time approximation was used did not match any of the τ_r values obtained from the ^{13}C data. While motions at the glycyl methylene position may be accounted for when models developed for the methylene and methine groups of synthetic polymers were used, the model does not apply to motions that occur at the peptide NH group.

Molecular Motion and the Organization of Cell Wall Polymers. The power of NMR spectroscopy as a probe of the arrangements of polymers which make up cellular structural

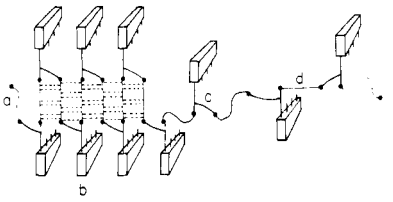

FIGURE 9: Possible arrangement of peptide chains between stacked rigid glycan planks in the *S. aureus* peptidoglycan network. Glycan strands are denoted by rectangles, which run perpendicular to the plane of the page, the stem and crossbar region of the peptide is denoted by γ, and the pentaglycine bridge chain is denoted by (—). Only one layer of the peptide chain is shown. Structures a and b correspond to the model proposed by Keleman & Rogers (1971).

components lies in the possibility of deducing the organization and mechanical properties of structural polymers from the nature of their molecular motions. It was of interest to consider to what extent the nature of chain motions of the pentaglycine bridge could be accounted for in terms of the models proposed for the arrangements of bacterial cell wall peptidoglycan.

Bacterial cell wall peptidoglycan consists of glycan strands of $\beta(1 \rightarrow 4)$-linked MurNAc and GlcNAc with average chain lengths of 15 disaccharide units (Rogers, 1970), which are interconnected by peptide chains attached to MurNAc residues. Several three-dimensional model building studies of peptidoglycan have been reported (Tipper, 1970; Keleman & Rogers, 1971; Braun et al., 1973; Oldmixon et al., 1974; Formanek et al., 1974), which all make use of inflexible chitinlike glycan strands linked by peptide chains in various folded conformations. Rogers has proposed (Keleman & Rogers, 1971) a model of *S. aureus* peptidoglycan that consists of stacked glycan strands interconnected by peptide chains that have been folded into extensively intramolecular hydrogen-bonded pseudo β sheets (Figure 9). The steric hindrance between adjacent pentaglycine bridges in such a tightly packed peptidoglycan network is expected to be so large that little segmental motion would be possible. If the packing of the glycan strands were stabilized by intramolecular hydrogen-bonding interactions involving the pentaglycine bridges, then the disruption of these interactions would be expected to either increase the mobility of the partially folded pentaglycine bridge chains or increase the fraction of unfolded chains. *Tight packing of cell wall polymers is not in agreement with the long T_1 found for the NMR resonance representing a sizable fraction of cell wall polymers. Intramolecular hydrogen bonding is not consistent with the fact that guanidine hydrochloride does not alter either the nature or the rate of the pentaglycine bridge chain segmental motions.* The assumption of tight packing of cell wall polymers is also not in agreement with the porosity of cell wall peptidoglycan (Scherrer & Gerhardt, 1971) and the lack of long-range order in the cell wall (Balyuzi et al., 1972).

A number of possible alternate arrangements for *S. aureus* cell wall peptidoglycan, which range from moderately separated glycan strands connected by flexible peptide chains (Figure 9b,c) to maximally separated glycan strands linked by fully extended peptide chains (Figure 9d), are possible. In these models, the motional freedom of the peptide chains is determined by the separation of the glycan strands rather than by noncovalent bonding interactions. This is consistent with the absence of an effect of guanidine hydrochloride on chain motions.

The combination of short average correlation times and a wide distribution of correlation times, which becomes even broader at high temperatures, distinguishes cell wall peptidoglycan from synthetic polymers in bulk and in solution. The nature of the chain motions in the synthetic polymers has been discussed by Schaefer (1973) and Herman & Weill (1975) who conclude that motion consists of rapid, short-range processes leading to partial loss of correlation of the C–H vector, followed by a slower, longer range process leading to the complete loss of correlation. The distribution narrows as the temperature increases, since greater thermal activity leads to greater independence of adjacent subunits and smaller difference between the time constants for the two types of motion. In bacterial cell wall peptidoglycan, the attachment of a flexible peptide chain to immobile glycan strands reduces the efficiency of the rapid process, leading to wide distribution of correlation times. Chain entanglements and filler particles have similar effects on synthetic bulk polymers (Schaefer, 1973). The increase in the width of distribution observed in cell wall peptidoglycan with increasing temperature can be rationalized by allowing the arrangements of the glycan strands to change with temperature in such a way as to reduce the efficiency of the rapid process. Rapid, short-range motions are expected to become more correlated and less effective as the pentaglycine chain is stretched. The swelling of the *S. aureus* cell wall at elevated temperatures found by Ou & Marquis (1972) is indeed consistent with an expansion of the peptidoglycan network and would be accompanied by extension of the peptide chain as shown in Figure 9 c,d. Changes in the separation of the glycan strands might be monitored by the distribution width parameter of the pentaglycine bridge, which is reflected in the T_2/T_1 ratio. Examination of the ^{15}N NMR data of normal- and thick-wall cells and isolated cell walls reveals differences in the packing of the glycan strands. The increase in T_2/T_1 ratios found when cell wall elongation is inhibited in the chloramphenicol-treated cells suggests that glycan strands are closer to each other in the thickened wall and that they spread apart during cell wall elongation in normal cells. The increase in the T_2/T_1 ratio on going from the intact cell to the isolated cell wall suggests that the glycan strands might be pulled apart as a result of cell turgor and tension on the cell wall and move closer together during the isolation of the cell wall. This is consistent with the elastic contraction of the cell wall, observed when cell turgor is reduced (Marquis, 1968).

Acknowledgments

We thank Magdah David for her technical assistance and Professor H. A. Scheraga and Dr. R. L. Somorjai for helpful discussions.

References

Abragam, A. (1961) *The Principles of Nuclear Magnetism*, Oxford University Press, London.

Balyuzi, H. H. M., Reaveley, D. A., & Burge, R. E. (1972) *Nature (London), New Biol. 235*, 252.

Braun, V., Gnirke, H., Henning, U., & Rehn, K. (1973) *J. Bacteriol. 114*, 1264.

Chien, J. C. W., & Wise, W. B. (1973) *Biochemistry 12*, 3413.

Christl, M., & Roberts, J. D. (1972) *J. Am. Chem. Soc. 94*, 4565.

Coley, J., Tarelli, E., Archibald, A. R., & Badiley, J. (1978) *FEBS Lett. 88*, 1.

Egan, W., Shingo, H., & Cohen, J. S. (1977) *Annu. Rev. Biophys. Bioeng. 6*, 383.

Formanek, H., Formanek, S., & Wawra, H. (1974) *Eur. J. Biochem. 46*, 279.

Ghuysen, J. M. (1968) *Bacteriol. Rev. 32*, 425.

Glushko, V., Lawson, P. J., & Gurd, F. R. N. (1972) *J. Biol. Chem. 247*, 3176.

Hawkes, G. E., Randall, E. W., & Bradley, C. H. (1976) *Nature (London) 257*, 767.
Heatley, F., & Begum, A. (1976) *Polymer 399*, 408.
Hermann, G., & Weill, G. (1975) *Macromolecules 8*, 171.
Irving, C. S., & Lapidot, A. (1975) *J. Am. Chem. Soc. 97*, 5945.
Irving, C. S., & Lapidot, A. (1978a) *Proc. Int. Conf. Stable Isot. Chem. Biol. Med., 3rd* (in press).
Irving, C. S., & Lapidot, A. (1978b) Abstracts, 45th Annual Meeting of the Israel Chemical Society, Haifa, Israel, June 1978, PC-2.
Keim, P., Vigna, R. A., Marshall, R. C., & Gurd, F. R. N. (1972) *J. Biol. Chem. 248*, 6104.
Keim, P., Vigma, R. A., Nigen, M., Morrow, S., & Gurd, F. R. N. (1974) *J. Biol. Chem. 249*, 4149.
Kelemen, M. V., & Rogers, H. J. (1971) *Proc. Natl. Acad. Sci. U.S.A. 68*, 992.
Lapidot, A., & Irving, C. S. (1977a) *J. Am. Chem. Soc. 99*, 5488.
Lapidot, A., & Irving, C. S. (1977b) *Proc. Natl. Acad. Sci. 74*, 1388.
Lapidot, A., & Irving, C. S. (1978) *Nuclear Magnetic Resonance Spectroscopy in Molecular Biology* (B. Pullman, Ed.) p 439, D. Reidel Publishing Co. Dorddrecht, Holland.
Lapidot, A., & Irving, C. S. (1979) *Biochemistry 18*, 704.
Levy, G. C., Axelson, D. E., Schwartz, R., & Hochmann, J. (1978) *J. Am. Chem. Soc. 100*, 410.
Llinas, M., & Wüthrich, K. (1978) *Biochim. Biophys. Acta 532*, 29.
Lyerla, J. R., Jr., & Levy, G. C. (1974) in *Topics in Carbon-13 NMR Spectroscopy* (Levy, G. C., Ed.) Vol. 1, p 79, Wiley, New York.
Lyerla, J. R., Jr., & Torchia, D. A. (1975) *Biochemistry 14*, 5175.
Lyerla, J. R., Jr., Horikawa, T. T., & Johnson, D. E. (1977) *J. Am. Chem. Soc. 99*, 2463.
Marowski, V., Posner, T., Loftus, P., & Roberts, J. D. (1977) *Proc. Natl. Acad. Sci. U.S.A. 74*, 1308.
Marquis, R. E. (1968) *J. Bacteriol. 95*, 775.
McVeigh, I., & Hobdy, C. J. (1952) *Am. J. Bot. 39*, 352.
Oldmixon, E. H., Glauser, S., & Higgins, M. L. (1974) *Biopolymers 13*, 2037.
Ou, L.-T., & Marquis, R. E. (1970) *J. Bacteriol. 101*, 92.
Ou, L.-T., & Marquis, R. E. (1972) *Can. J. Microbiol. 18*, 623.
Rogers, H. J. (1970) *Bacteriol. Rev. 34*, 194.
Rogers, H. J. (1974) *Ann. N.Y. Acad. Sci. 235*, 29.
Rogers, H. J., & Forsberg, C. W. (1971) *J. Bacteriol. 108*, 1235.
Salton, M. R. (1964) *The Bacterial Cell Wall*, American Elsevier, New York.
Schaefer, J. (1973) *Macromolecules 6*, 882.
Schaefer, J. (1974) in *Topics in Carbon-13 NMR Spectroscopy* (G. C. Levy, Ed.) p 150, Wiley, New York.
Scherrer, R., & Gerhardt, P. (1971) *J. Bacteriol. 197*, 718.
Schoenheimer, R., & Ratner, S. (1938) *J. Biol. Chem. 127*, 301.
Shockman, G. D., Danen-Moore, L., & Higgins, N. L. (1974) *Ann. N.Y. Acad. Sci. 235*, 161.
Spizizen, J. (1958) *Proc. Natl. Acad. Sci. U.S.A. 44*, 1072.
Tancrede, P., Deslauriers, R., McGregor, W. H., Ralston, E., Sarantakis, D., Somorjai, R. L., & Smith, I. C. P. (1978) *Biochemistry 17*, 2903.
Tipper, D. J. (1970) *Int. J. Syst. Bacteriol. 20*, 361.
Torchia, D. A., & Vanderhart, D. L. (1976) *J. Mol. Biol. 104*, 315.
Torchia, D. A., Hasson, M. H., & Hascall, V. C. (1977) *J. Biol. Chem. 252*, 3617.